Transport Current Dependence of the Hysterisis Loss in Silver Sheathed BSCCO-2212 Conductors

Herman. Hemmes*, Martin J. Woudstra*, Herman H.J. ten Kate* and Johannes Tenbrink**

* Applied Superconductivity Centre, Department of Applied Physics, University of Twente, P.O.Box 217, NL-7500 AE Enschede, the Netherlands

** VacuumSchmelze GmbH, Grünerweg 37, D-6450 Hanau 1, Germany

A technique is described to study the critical current density and penetration field associated with the transport current in a silver sheathed BSCCO conductor. A transport current flowing in a conductor in a varying magnetic field will only influence magnetisation currents that are in competition with the transport current, i.e. currents that use the same path. By measuring the transport current dependence of the magnetisation loss information can be obtained on the related critical current and penetration field. The combination of these two quantities contains information about the geometry of the current distribution and can be used to test different models for the current distribution in BSCCO conductors.

INTRODUCTION

For future high current application of high T_c superconductors knowledge and control of the electric and magnetic properties of the materialsis essential. Recently considerable progress has been made in the preparation of Ag sheathed BiSrCaCuO conductors. One of the problems encountered in analysing the properties of these materials is the large discrepancy between the critical current densities obtained from transport ($J_{c,t}$) and magnetic ($J_{c,m}$) measurements as a result of the granular structure of the superconductor. Since $J_{c,t}$ is generally much smaller than $J_{c,m}$, one of the major issues is to identify the part of the superconducting cross section that carries the transport current. Generally it is believed that the transport current is carried in the textured region near the interface with the silver matrix. The transport critical current can be influenced by disturbances in the superconducting path that could be so small that they would hardly influence the magnetic properties, even in the absence of a granular structure. The presence of the granular micro-structure makes the analysis of magnetisation data and the associated losses even more difficult in terms of inter-grain shielding currents that can be related to the transport current.

In this paper a technique is presented to study the effect of inter-grain contributions to the magnetic losses. The technique is based on the influence of a dc transport current on the magnetisation of a superconductor in an applied magnetic field. When the transport current approaches the critical current, the magnetisation and the corresponding losses will go to zero. Since the transport current hardly influences the shielding currents in the grains, it will have no effect on the related losses. By measuring the magnetic hysteresis losses as a function of transport current and field amplitude, information is obtained about the transport critical current density and the related penetration field of the superconductor, even when the losses from the grains cannot be neglected. The penetration field and critical current density together also supply information about the geometry of the current distribution.

THEORY

An analytical model is constructed for the description of the transport current dependence of the magnetisation loss for a filament in perpendicular field. The model consists of a phenomenological interpolation between an analytical expression for losses in the absence of transport current and an expression for large field amplitudes derived from the transport current dependence of the saturated magnetisation [1,2]. The presence of the transport current I_t has essentially two effects. First the cross

section available to shielding currents reduces, which is described by an $1\text{-}i^2$ term, where $i = I_t/I_c$. Second the shape of the shielding current distribution is influenced, which is modelled by a current dependent penetration field $B_p(i)$. The loss per unit volume per cycle, $Q(i,B_a)$, for a field with amplitude B_a is given by

$$Q(i,B_a) = \begin{cases} \frac{4}{3\mu_0} B_a^2 \left(2\beta(i) - \beta(i)^2\right) \frac{1-i^2}{f(i)} & \beta \le 1 \\ \frac{4}{3\mu_0} B_a^2 \left(\frac{2}{\beta(i)} - \frac{1}{\beta(i)^2}\right) \frac{1-i^2}{f(i)} & \beta \ge 1 \end{cases} \quad (1)$$

where $\beta(i) = B_a/B_p(i)$, $B_p(i) = B_p(0)f(i)$, $B_p(0) = \frac{2}{\pi}\mu_0 J_c R_f$, $f(i) = (1-i)(1+i/2)$, $I_c = J_c \pi R_f^2$ and $i = I_t/I_c$, with $I_t(I_c)$ the transport(critical) current, J_c the critical current density and R_f the filament radius. Because the form of equation 1 does not take into account that the dependence on the applied magnetic field changes it will describe only a limited range of field amplitudes correctly. This range can be adjusted by changing the current dependent part $f(i)$ of the penetration field. In order to 'fit' $f(i)$ to the field range of interest, the transport current dependence of the magnetisation loss was calculated numerically. For this the formalism described in [1] was used. Figure 1 shows a comparison of the results obtained numerically and with the analytical model for $f(i)$ as given above. Because the loss increases very rapidly with increasing field amplitude the losses are scaled to those at zero transport current. It is useful to note that the curves in figure 1 depend only on scaled quantities and are therefore independent of the absolute values of J_c , R_f and B_a. Note that the loss is most sensitive to the transport current for magnetic field amplitudes smaller than the penetration field. For field amplitudes larger than the penetration field the shape of the loss curve changes only slightly. Information about the penetration field can therefore only be obtained from curves for small field amplitudes.

EXPERIMENTAL

Silver sheathed BSCCO-2212 wires with 19 filaments are produced at VacuumSchmelze GmbH by the powder in tube method. After drawing the wire to the final diameter (1.2 mm) pieces of ~1 m length are wound on an AISI 304 stainless steel tube with an outer diameter of 43 mm. A glass dummy wire between the sample turns is used in order to reduce the effect of the self field. It also provides support to the sample during heat treatment. After heat treatment the sample is transferred to a glass epoxy tube and is glued with STYCAST 2850 epoxy. Copper strips are used as current contacts as shown in figure 2. Eight voltage taps are connected to the sample. All soldering connections are made using non-superconducting SnAg solder.

The sample holder is inserted in a fully superconducting set-up for magnetisation measurements that also allowes voltage-current measurements. The pickup set acts a flux transformer, where the current is proportional to the magnetic moment of the sample. The magnitude of the induced current is measured by placing a Hall-probe in the sensing coil of the flux transformer. Because the flux transformer acts as a perfect integrator, losses can be measured at quasi-zero frequency. All measurements presented here were done at 20 mHz. The whole set-up is placed in two concentric superconducting magnets, a 7 T DC magnet and a 0.6 T AC magnet for measuring the frequency dependence.

RESULTS AND DISCUSSION

Figure 3 shows the transport current dependence of the magnetisation loss, scaled to the zero transport current value, for several field amplitudes, measured on a 19 filament Ag sheated BSCCO-2212 wire. For the smallest amplitude two maxima can be observed. When comparing the data to the theoretical curves, two major contributions to the loss can be identified for transport currents below 30 A. Also a tail at higher currents is observed. From the shape of the data two critical currents can be identified: ~15 A and ~30 A. Voltage-Current (VI) charcateristics are measured over several sections of the sample. From the VI-curves no indications are found for the presence of two megnetic subsystems. The largest magnetically determined $I_{c,m}$ is consistent with the $I_{c,t}$ of the best section of the sample at E = 0.2 μV/m. Because for a section with worse properties no reliable extrapolation to low electric fields could be made, it was not

possible to positively relate the smaller $I_{c,m}$ to the electrical measurements.

Fitting the measured data with two contribution, described by equation 1, is not possible. A background is needed below 30 A. If the tail above 30 A arises from a part of the sample with a broad distribution of critical currents, a contribution will also be present for currents below 30 A. For small currents it can be shown that the B_a and i dependence of the loss does not change when equation 1 is convoluted with a distribution function. When equation 1, with an 'average' current density and filament radius, is used to model the background it will scale correct with B_a and i for smaller currents.

A fit to the measured data assuming two contributions and a background resulted in the lines shown in figure 3. The fit parameters: J_c, R_f and the volume fraction for the two dominant contributions are listed in Table 1, together with the derived penetration field at zero transport current.

Table 1 Parameters that fit the model to the measured data in figure 3.

	J_c (A/m^2)	R_f (μm)	volume fraction	$B_p(0)$(mT)	I_c(A)
1	4.4 10^7	77	0.29	2.7	15
2	6.9 10^7	82	0.48	4.6	28

The sample is also analysed by optical and scanning electron microscopy. An average filament radius of 85 μm is found, which is close to the value obtained for the second contribution. However, the filament radius of the first contribution is to small. In the longitudinal cross section, shown in figure 4, a large number of voids can be observed. Since voids effectively reduce the cross section of the filament, this suggest that the 'low' I_c contribution could be related to the volume fraction containing the voids and the 'high' I_c to the volume fraction with solid cross section.

For a solid filament the maximum in Q/B_a^2 occurs when B_a is equal to the penetration field B_{ps}. When a hole is introduced in the filament the field dependence of the loss curve changes and the penetration field B_{ph} lies below the maximum in the Q/B_a^2 curve [1]. If the loss curve of a hollow filament is fitted with a solid filament model the resulting penetration field will be a measure of the position of the maximum in the Q/B_a^2 curve and therefore be larger than the actual B_{ph}. Since the critical current is independent of the model, the filament radius obtained from the fit will be to small. A simple analytical model for a hollow filament provides a relation between the penetration field and the maximum of the Q/B_a^2 curve. This allows for an estimate of the actual B_{ph}. When B_{ps} is corrected to B_{ph}, the dimensions of the hollow filament obtained are in qualitative agreement with the actual dimensions of the voids observed in figure 4. Another consquence of the hollow filament geometry is an increase in J_c, which becomes comparable to that of the second contribution.

Presently it seems that the experimental results can be explained in a consistent way by assuming two sub-systems in the filaments with different geometry. However, it should be pointed out that one has to be careful with the geometrical interpretation of the data since we already saw that the wrong geometry (solid filament) can describe the results remarkably well.

CONCLUSION

It is shwon that the transport current dependence is potentially a valuable tool for studying the loss mechanisms, and structure of the BSCCO conductor. The experimental data clearly shows the presence of two major contributions to the losses, whereas the VI-characteristics showed no evidence of this. The two contributions were tentatively explained by the presence of voids in the filaments, creating two different current distributions. The model fits suggest that the superconductor has a homogeneous J_c over the whole cross section. However, more work has to be done in order to determine the uniqueness of the results. By combining the transport current dependence of magnetisation losses with VI-chararcteristics and microscopic analaysis a better insight in the superconducting properties of the filaments can be obtained.

REFERENCES

[1] R.A. Hartmann, A Contribution to the Understanding of AC Losses in Composite Superconductors, PhD thesis, University of Twente (1989)

[2] H. Hemmes, M.J. Woudstra, H.H.J. ten Kate and J. Tenbrink, in preparation

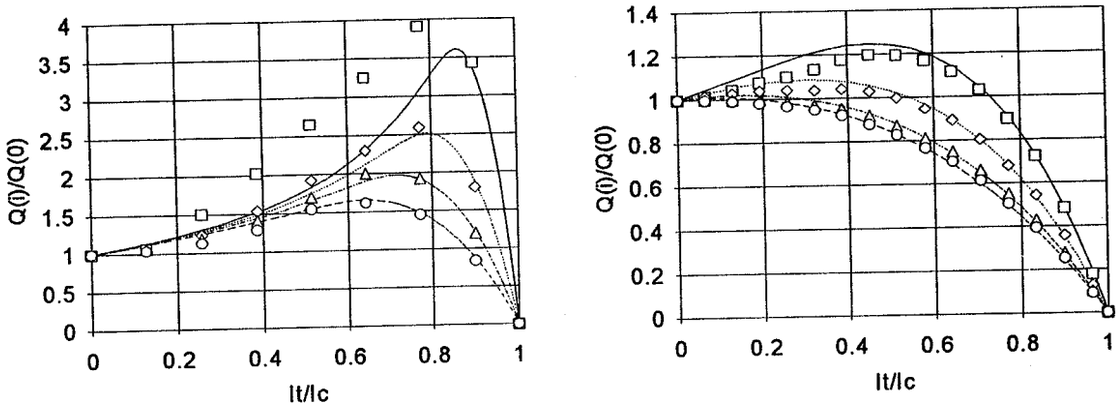

Figure 1. Transport current dependence of the magnetisation loss for different values of the applied magnetic field. The symbols and lines denote the numerical and analytical results. The field amplitudes, scaled to the penetration field for the different curves are: Left: B_a/B_p = 0.2 (solid,□), 0.3 (dot,◊), 0.4 (dash-dot,Δ), 0.5 (dash,○). Right: B_a/B_p = 0.75 (solid,□), 1.0 (dot,◊), 1.5 (dash-dot,Δ), 2.0 (dash,○).

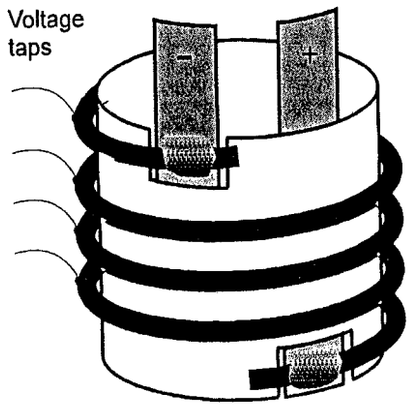

Figure 2. Coil sample with current contacts and voltage taps.

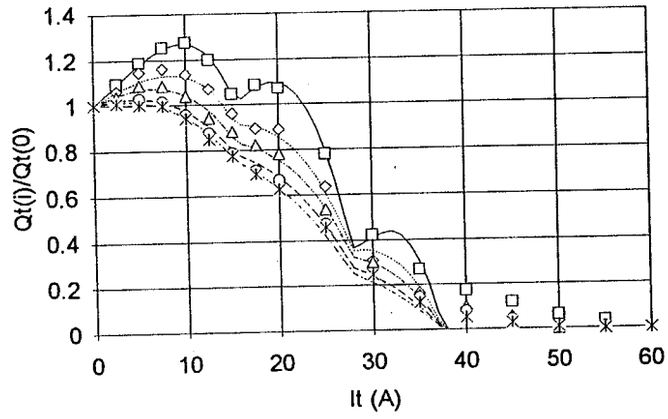

Figure 3. Scaled values of measured (symbols) and calculated (lines) losses as a function of transport current for several field amplitudes: 2 (□), 3 (◊), 4 (Δ), 6 (○) and 8 (×) mT

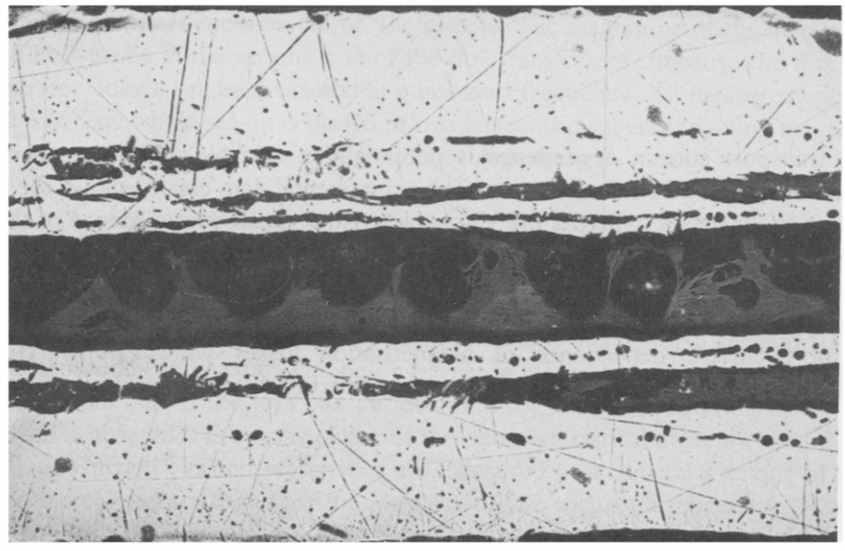

Figure 4. Longitudinal section of a BSCCO-2212 filament in the silver matrix.